This article has been accepted for publication in a future issue of this journal, but has not been fully edited. Content may change prior to final publication. Citation information: DOI 10.1109/TSG.2017.2745494, IEEE Transactions on Smart Grid

A Forecasting-Residual Spectrum Analysis Method for Distinguishing Forced and Natural Oscillations

Mohammadreza Ghorbaniparvar, *Student Member, IEEE*, Ning Zhou, *Senior Member, IEEE*, and Xiaohua Li, *Senior Member, IEEE*, Dan Trudnowski, *Fellow, IEEE*, Ruichao Xie, *Student Member, IEEE*

***Abstract*—In order to effectively implement remedial reactions to mitigate the negative impacts of oscillations on a power grid, it is essential for system operators to timely and accurately determine whether an observed oscillation is a natural oscillation or a forced oscillation. Using phasor measurement unit (PMU) data, this paper proposes a residual spectral analysis (RSA) method to distinguish forced oscillations and natural oscillations. The proposed RSA method uses forecasting models with various lead times to forecast the current PMU data based on the past PMU data. The spectra of the forecasting residuals are shown to have different properties when the PMU data have forced or natural oscillations. Support vector machines (SVMs) are applied to the residuals to classify the oscillations. This paper develops an algorithm for implementing the RSA method, and demonstrates its superior performance via extensive simulations over the 48-machine model. Simulations show that it can distinguish the oscillations more accurately than an existing method and work reliably even when the frequency of forced oscillations is close to that of natural oscillations.**

***Index Terms*— phasor measurement units, power system dynamics, oscillations, forecasting, spectral analysis.**

I. Introduction

TO ENSURE the stability and reliability of a power grid, it is critical to detect and distinguish oscillations in time. Oscillations can cause numerous problems such as system breakups [1], decreased life expectancy of devices [2], and flickering light which is annoying to human eyes [3]. Based on their root causes, oscillations can be divided into two categories: forced oscillations and natural (or free) oscillations. Forced oscillations are incurred by external periodic perturbations [12-17], whereas natural oscillations are caused by intrinsic natural interactions among dynamic components [4-11]. These oscillations should be studied thoroughly so that cause-effect knowledge can be established to support proper remedial reactions.

The remedies for natural oscillations and forced oscillations are different. Natural oscillations can be mitigated by improving damping. It often calls for reducing tie line flows to change operation points [15], and adding damping control systems such as power system stabilizers (PSS) [18], [19]. For example, to improve the damping of an inter-area oscillation (a natural oscillation) in the Western Electricity Coordinating Council (WECC) system, the Bonneville Power Administration (BPA) established Dispatcher Standing Order 303 to reduce tie-line flow when the damping of interarea modes is dangerously low. In contrast, to suppress forced oscillations, the source of oscillations should be identified and detached from systems [20]. As it has been reported in [21][22], treating forced oscillations as natural oscillations can mislead the estimation methods and subsequent control strategies. As such, it is important to distinguish forced and natural oscillations.

Phasor measurement units (PMU) are being deployed in the modern power grid and providing highly synchronized data which carry invaluable information about stability of power grids. Oscillation analysis using PMU data is an integral part of smart grid to improve operators' situational awareness. Some initial studies have been carried out to distinguish forced and natural oscillations based on PMU data [23-25, 30]. Liu et al. in [23] used support vector machines (SVMs) to extract the features of oscillations. The increasing amplitude of natural oscillations was used to distinguish them from forced oscillations. On the other hand, since the accuracy of this algorithm has direct relationship with the envelope size, there is a question on whether the algorithm can work in real-time scenarios. Using the noise response and the harmonic nature of oscillations, Xie et al. in [24] proposed a spectral method to distinguish forced oscillations from natural oscillations. Yet, it was found that the performance may degrade when the frequency of forced oscillations is close to the system's mode frequency. The Wang et al. in [25] proposed an algorithm that uses power spectral density (PSD) and kurtosis to distinguish the oscillations. Nevertheless, as explained in [17], a large amount of time is required in order to get an accurate PSD estimation from PMU data. This method may be suitable for off-line applications only.

It is still a challenge to develop robust methods for distinguishing forced and natural oscillations, especially when

This work is supported in part by the Research Foundation for the State University of New York.

M. Ghorbaniparvar, N. Zhou, and X. Li are with Department of Electrical and Computer Engineering, State University of New York at Binghamton, Binghamton, NY 13902, USA (emails: {mghorba1, ningzhou, xli} @binghamton.edu).

D. Trudnowski and R. Xie are with Montana Tech of the University of Montana, Butte, MT 59701, USA (emails: {DTrudnowski, RXie} @mtech.edu)

This article has been accepted for publication in a future issue of this journal, but has not been fully edited. Content may change prior to final publication. Citation information: DOI 10.1109/TSG.2017.2745494, IEEE Transactions on Smart Grid

the frequency of forced oscillations is close to the system's mode frequency. To address this challenge, this paper proposes a residual spectral analysis (RSA) method, which distinguishes oscillations based on the forecasting-residuals of a class of forecasting models using SVMs. The proposed method is shown to successfully distinguish forced and natural oscillations even when the frequency of forced oscillations is close to the natural oscillation frequencies.

The rest of the paper is organized as follows. Section II introduces the mathematical model for forced and natural oscillations. The RSA method is proposed in Section III. In Section IV, this method is evaluated by simulations. Conclusions are drawn in Section V.

II. Oscillation Models

To study and analyze small-signal stability of a power system, dynamic models are often linearized around an equilibrium operation point. It was shown in [18] that small deviations in the power system can be modeled by a set of linear differential equations as

$$\dot{x}(t) = Ax(t) + b_1 f(t) + \sum_{k=1}^{M} b_{2k} q_k(t) \tag{1}$$

where $A \in R^{N\times N}$ is the state transition matrix, $x(t) \in R^{N\times 1}$ is the system state vector, t is time, $f(t)$ is the scalar source of forced oscillations, the scalar inputs $q_k(t)$, $k = 1,\cdots,M$, denote white Gaussian noise (WGN), $b_1 \in R^{N\times 1}$ is the gain of the forced oscillation input and $b_{2k} \in R^{N\times 1}$ is the noise gain.

The solution to (1) gives the system's dynamic response, which consists of three components, i.e., ambient, transient and forced components. The ambient component is the system's response to low-magnitude random load variations [26]. The transient component is usually caused by an abrupt change, such as line fault, or generation tripping. The forced component is the system's response to external periodic injections, such as malfunction controllers [27]. Based on the three components, the solution to (1) can be represented by

$$\begin{aligned} x_r(t) = \sum_{i=1}^{N} u_{ir} v_i x(0) e^{\lambda_i t} + \sum_{m=-\infty}^{\infty} \left(\sum_{i=1}^{N} u_{ir} v_i b_1 e^{\lambda_i t} \right) \otimes A_m e^{jm\omega_0 t} \\ + \sum_{k=1}^{M} \left(\sum_{i=1}^{N} u_{ir} v_i b_{2k} e^{\lambda_i t} \right) \otimes q_k(t) \end{aligned} \tag{2}$$

where $x_r(t)$ is the r^{th} element of the vector $x(t)$, $x(0)$ is the initial state vector which represents a post-fault transient, $\otimes$ is the convolution operator and $j = \sqrt{-1}$. In addition, following [24], $u_i \in C^{N\times 1}$ and $v_i \in C^{1\times N}$ denote the left and right eigenvectors corresponding to the eigenvalue λ_i of A, respectively, and u_{ir} is the r^{th} element of vector u_i. Furthermore, in (2) the source of forced oscillation $f(t)$ is modeled by its Fourier series harmonics as

$$f(t) = \sum_{m=-\infty}^{\infty} A_m e^{jm\omega_0 t} \tag{3}$$

where ω_0 is the angular frequency of the forced oscillations, and A_m is a complex number whose angle determines the phase of the m[th] harmonic. Note that non-periodic external disturbances are not modeled as forced oscillations because they do not have sharp peaks in their PSD.

To study the features of natural and forced oscillations, two special cases can be considered. In the first case, there is only natural oscillation, which is caused by a lightly damped mode λ_n. In the second case, there is only forced oscillation at $m\omega_0$, and natural oscillation is absent because all the system modes are well-damped.

Natural-oscillation case: Consider the N modes λ_i in (2). Assume that only the mode n is lightly-damped and all the other $N-1$ modes are well-damped. In this case, one has

$$\lambda_i = \sigma_i + j\omega_i, \qquad i = 1,\cdots,N \tag{4}$$

with $\sigma_i << 0$ for $i \neq n$ and $\sigma_n \approx 0$. Their corresponding damping ratios are $\zeta_i = \frac{-\sigma_i}{\sqrt{\sigma_i^2 + \omega_i^2}} >> 0\%$ and $\zeta_n \approx 0\%$. Because the forced oscillation component $f(t)$ is assumed zero, (2) becomes

$$\begin{aligned} \hat{x}_r(t) = u_{nr} v_n x(0) e^{j\omega_n t} \quad &\Rightarrow \text{Transient} \\ + \sum_{k=1}^{M} \left(u_{nr} v_n b_{2k} e^{j\omega_n t} \right) \otimes q_k(t) \quad &\Rightarrow \text{Noise } z_r(t) \\ + \sum_{\substack{i=1 \\ i\neq n}}^{N} \sum_{k=1}^{M} \left(u_{ir} v_i b_{2k} e^{\lambda_i t} \right) \otimes q_k(t) \quad &\Rightarrow \text{Residue noise} \end{aligned} \tag{5}$$

Because $\sigma_n \approx 0$, the noise $z_r(t) = \sum_{k=1}^{M} \left(u_{nr} v_n b_{2k} e^{j\omega_n t} \right) \otimes q_k(t)$ is the convolution of a sinusoidal signal with the random noise, which was named "random sinusoid" response in [24]. The noise $z_r(t)$ and the transient response dominate in (5) because the residue noise is very small.

Forced-oscillation case: Assume that the system is asymptotically stable and all the modes are well-damped with $\sigma_i << 0$, $i = 1,\cdots,N$. The response (2) becomes

$$\begin{aligned} \hat{x}_r(t) = \sum_{m=-\infty}^{\infty} \left(\sum_{i=1}^{N} u_{ir} v_i b_1 e^{\lambda_i t} \right) \otimes A_m e^{jm\omega_0 t} \quad &\Rightarrow \text{Forced} \\ + \sum_{i=1}^{N} \sum_{k=1}^{M} \left(u_{ir} v_i b_{2k} e^{\lambda_i t} \right) \otimes q_k(t) \quad &\Rightarrow \text{Residue noise} \end{aligned} \tag{6}$$

Obviously, the forced item dominates in (6) since the residue noise is very small.

Comparing the two cases (5) and (6), one can observe that the ***natural oscillation case*** involves the special "random sinusoid" which is absent in the ***forced oscillation case***. Therefore, whether the "random sinusoid" $z_r(t)$ presents in $x_r(t)$ can be used to distinguish forced oscillations from natural oscillations.

III. Distinguish Forced and Natural Oscillations

This section builds a forecasting model and uses the spectra of the forecasting residuals to detect the random sinusoid and

This article has been accepted for publication in a future issue of this journal, but has not been fully edited. Content may change prior to final publication. Citation information: DOI 10.1109/TSG.2017.2745494, IEEE Transactions on Smart Grid

thus to distinguish natural and forced oscillations.

Consider the generic forecasting model shown in Fig. 1, which uses $x[k-N_T]$ to forecast $x[k]$, where N_T is the lead time of forecasting. Note that discrete time signals are considered, where $x[k]=x(kT_s)$ with the sampling interval T_s.

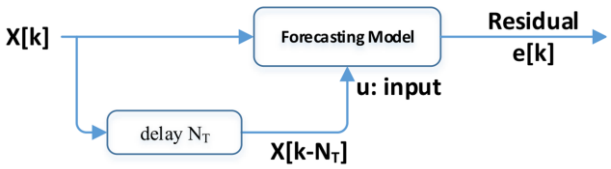

Fig. 1. A simple forecasting model that uses past samples $x[k-N_T]$ to forecast $x[k]$ with forecasting residual $e[k]$.

The residual of forecasting is

$$e[k]=x[k]-g\left(x[k-N_T],\cdots,x[k-N_T-D]\right) \tag{7}$$

where $g(x)$ denotes a forecasting function that uses $D+1$ past samples N_T steps ahead to forecast $x[k]$.

A. Forecasting Residual in Natural-oscillation Case

When a natural oscillation is observed, the noise $z_r(t)$ and the transient response in (5) dominate the system response $\hat{x}_r(t)$. Because the transient response is a pure or slightly attenuated sinusoidal signal, it can be well forecasted with very small residuals. The forecasting residuals are dominated by $z_r(t)$. Therefore, to simplify notation, one can focus only on $z_r(t)$ when analyzing the forecasting residuals. Specifically, it can be derived from (5) that

$$\begin{aligned} z_r[k] &= \sum_{m=1}^{M}\left(u_{nr}v_n b_{2m} e^{j\omega_n kT_s}\right)\otimes q_m[kT_s] \\ &= \sum_{m=1}^{M} e^{j\omega_n kT_s}\otimes\left(u_{nr}v_n b_{2m} q_m[kT_s]\right) \\ &= e^{j\omega_n kT_s}\otimes\sum_{m=1}^{M}\left(u_{nr}v_n b_{2m}\right) q_m[kT_s] \\ &= e^{j\omega_n kT_s}\otimes Q[k] \end{aligned} \tag{8}$$

In (8), Q[k] is defined by (9).

$$Q[k]=\sum_{m=1}^{M}\left(u_{nr}v_n b_{2m}\right) q_m[kT_s]. \tag{9}$$

Because the items $q_m[kT_s]$ are WGN that are independent from each other for different *m*, $Q[k]$ is also WGN.

As the power system is a causal system, $z_r[k]$ depends on $Q[l]$ for $l\le k$ only. The convolution in (8) can be decomposed into two items as in (10).

$$\begin{aligned} z_r[k] &= \sum_{l=-\infty}^{k} e^{j\omega_n(k-l)T_s}Q[l] \\ &= \sum_{l=-\infty}^{k-N_T} e^{j\omega_n(k-l)T_s}Q[l] \qquad \Rightarrow \text{Item 1} \\ &\quad + \sum_{l=k-N_T+1}^{k} e^{j\omega_n(k-l)T_s}Q[l] \qquad \Rightarrow \text{Item 2} \end{aligned} \tag{10}$$

Similarly, the explanatory variable of the forecasting model $z_r[k-N_T-d]$, $d=0,\cdots,D$, can be represented by (11).

$$\begin{aligned} z_r[k-N_T-d] &= e^{j\omega_n(k-N_T-d)T_s}\otimes Q[k-N_T-d] \\ &= \sum_{l=-\infty}^{k-N_T} e^{j\omega_n(k-N_T-d-l)T_s}Q[l] \\ &= e^{-j\omega_n(N_T+d)T_s}\sum_{l=-\infty}^{k-N_T} e^{j\omega_n(k-l)T_s}Q[l] \end{aligned} \tag{11}$$

Note that the last item (with the summation sign) in (11) is exactly *Item 1* in (10). This means that $z_r[k-N_T-d]$ is correlated to $z_r[k]$ in term of *Item 1* of (10). On the other hand, $z_r[k-N_T-d]$ is uncorrelated to *Item 2* of (10) because $Q[k]$ is WGN. Therefore, when using the random sinusoidal $\{z_r[k-N_T],\cdots,z_r[k-N_T-D]\}$ to forecast the random sinusoidal $z_r[k]$, the residuals shall be dominated by *Item 2* of (10). For example, with $D=0$ and the optimal forecasting function $g(x)=e^{j\omega_n N_T T_s}x$, we have

$$e[k]\approx\sum_{l=k-N_T+1}^{k} e^{j\omega_n(k-l)T_s}Q[l]. \tag{12}$$

In general, $D>0$ can be used for more effective forecasting.

In addition, (12) can be viewed as the convolution of the white noise $Q[k]$ and the windowed sinusoidal signal $e^{j\omega_n kT_s}$. Equation (12) can be written as

$$\begin{aligned} e[k] &\approx \sum_{m=0}^{N_T-1} e^{j\omega_n mT_s}Q[k-m] \\ &= \left(\left(u[k-N_T+1]-u[k+1]\right)e^{j\omega_n kT_s}\right)\otimes Q[k] \end{aligned} \tag{13}$$

where $u[k-N_T+1]-u[k+1]$ defines a rectangle window of size N_T with step function $u[k]=\begin{cases}1, & \text{for } k\ge 0\\ 0, & \text{for } k<0\end{cases}$.

B. Forecasting Residual in Forced-oscillation Case

When a forced oscillation is observed, the *Forced* item in (6) dominates the system response. In this case, skipping the small residue noise for notational simplicity, one can obtain

$$\begin{aligned} \hat{x}_r[k] &\approx \sum_{m=-\infty}^{\infty}\left(\sum_{i=1}^{N} u_{ir}v_i b_1 e^{\lambda_i kT_s}\right)\otimes A_m e^{jm\omega_0 kTs} \\ &= \sum_{m=-\infty}^{\infty}\sum_{l=-\infty}^{\infty}\left(\sum_{i=1}^{N} u_{ir}v_i b_1 e^{\lambda_i lT_s}\right)A_m e^{jm\omega_0(k-l)Ts}. \end{aligned} \tag{14}$$

Similarly, the explanatory variable is

This article has been accepted for publication in a future issue of this journal, but has not been fully edited. Content may change prior to final publication. Citation information: DOI 10.1109/TSG.2017.2745494, IEEE Transactions on Smart Grid

$$\hat{x}_r[k-N_T-d] \approx \sum_{m=-\infty}^{\infty}\sum_{l=-\infty}^{\infty}\left(\sum_{i=1}^{N} u_{ir}v_i b_1 e^{\lambda_i l T_s}\right) A_m e^{jm\omega_0(k-l)Ts} e^{-jm\omega_0(N_T+d)T_s} \quad (15)$$

If the forced oscillation $f(t)$ has just a single frequency $m\omega_0$, then $\hat{x}_r[k-N_T]$ can be used to forecast $\hat{x}_r[k]$ perfectly. In this case, $D=0$ and the optimal forecasting function is $g(x)=e^{jm\omega_0 N_T T_s}$. In general, $f(t)$ can be approximated by a few harmonics of large magnitudes. If there are M such harmonics, then with $D \geq M-1$, perfect forecasting can still be achieved with linear forecasting function $g(\hat{x}_r[k-N_T-d]) = \sum_{d=0}^{D} g_d \hat{x}_r[k-N_T-d]$. From (14) and (15), it is easy to see that the optimal coefficients g_d is the solution to the following linear equation system

$$\begin{bmatrix} a_{00} & \cdots & a_{0D} \\ \vdots & & \\ a_{M-1,0} & \cdots & a_{M-1,D} \end{bmatrix} \begin{bmatrix} g_0 \\ \vdots \\ g_D \end{bmatrix} = \begin{bmatrix} 1 \\ \vdots \\ 1 \end{bmatrix}, \quad (16)$$

where $a_{md} = e^{-j(m+1)\omega_0(N_T+d)T_s}$. In both cases, the forecasting residuals are just the residual noises in $\hat{x}_r[k]$ and $\hat{x}_r[k-N_T-d]$.

C. Spectra Analysis of Forecasting Residuals

First, if there is natural oscillation with frequency ω_n in the PMU data $x_r[k]$, then the forecasting residual is (13). In the frequency domain, the spectra of the rectangle function $u[k-N_T+1]-u[k+1]$ is a *sinc* function, whose peak value is proportional to the window length N_T. The WGN $Q[k]$ has a flat spectra while the sinusoidal function $e^{j\omega_n kT_s}$ has a peak at ω_n. The multiplication operation in the time domain can be translated into the convolutions in the frequency domain. Therefore the spectrum of the residuals in (13) has a peak at ω_n whose amplitude is proportional to the lead time N_T of the forecasting model. Because the PSD at ω_n dominates the residual power, according to (9) and (12), the peak magnitude is approximately

$$E\left[|e[k]|^2\right] = N_T \sum_{m=1}^{M} |u_{nr}v_n b_{2m}|^2 E\left[|q_m[kT_s]|^2\right], \quad (17)$$

where $E\left[|q_m[kT_s]|^2\right]$ is the WGN power.

Therefore, the PSD at frequency ω_n is N_T times of the noise power, while the PSD at other frequencies is just as small as the noise power. This not only shows that the spectra have a peak at the oscillation frequency ω_n, but also shows that this peak is linearly increasing with the forecasting lead time N_T. As a result, both the magnitude of the residual spectra and the slope of a series of residual spectra can be used to detect natural oscillations.

Second, if there is no oscillation in the PMU data $x_r[k]$, then from (2), one may have

$$x_r[k] = \sum_{m=1}^{M}\left(\sum_{i=1}^{N} u_{ir}v_i b_{2m} e^{\lambda_i kT_s}\right) \otimes q_m[kT_s] \quad (18)$$

Note that because all the modes $\lambda_i = \sigma_i + j\omega_i$ are well-damped with $\sigma_i << 0$, the transient response involving $x(0)$ can be omitted and the power of $x_r[k]$ is very small.

Similar to the analysis of (8)-(13), one can find the forecasting residual as

$$e[k] \approx \sum_{m=1}^{M}\left(\sum_{i=1}^{N} u_{ir}v_i b_{2l}\left(u[k-N_T+1]-u[k+1]\right)e^{\lambda_i kT_s}\right) \otimes q_m[kT_s]. \quad (19)$$

The PSD has very small peaks at mode frequencies ω_i, whose peak magnitude can be described approximately by the power of $e[k]$ (for each mode) as

$$E\left[|e[k]|^2 \,\middle|\, \text{mode } i\right] = \sum_{m=1}^{M} |u_{ir}v_i b_{2m}|^2 E\left[|q_m[kT_s]|^2\right]. \quad (20)$$

Comparing (20) with (17), it is clear that natural oscillation leads to a much higher peak in the residual spectra.

Next, if there is a forced oscillation with frequency $m\omega_0$ only, since the forced oscillation can be perfectly removed through forecasting, the forecasting residual is just noise, i.e.

$$\begin{aligned} e[k] \approx & \sum_{m=1}^{M}\left(\sum_{i=1}^{N} u_{ir}v_i b_{2l}\left(u[k-N_T+1]-u[k+1]\right)e^{\lambda_i kT_s}\right) \otimes q_m[kT_s] \\ & + (e^{\lambda_i N_T T_s} - e^{jm\omega_0 N_T T_s}) \sum_{m=1}^{M}\left(\sum_{i=1}^{N} u_{ir}v_i b_{2l} e^{\lambda_i (k-N_T)T_s}\right) \otimes q_m[(k-N_T)T_s] \end{aligned} \quad (21)$$

where the first item is due to the noise in $x_r[k]$ while the second item is due to the noises in both $x_r[k]$ and $x_r[k-N_T]$. In this case, the PSD of the residual becomes similar to the no-oscillation case (19) and (20). The spectra will not have a significant peak at the forced oscillation frequency, which is different from the natural oscillation case.

If using D explanatory variables in the forecasting model, the spectra magnitude increases by D folds. Nevertheless, by increasing the forecasting lead time to $N_T >> D$, the natural oscillation peak can still be much more significant. More importantly, the slope of the natural oscillation peak over N_T is still a unique feature for natural oscillations.

Finally, if natural and forced oscillations happen simultaneously, then the residual depends on the power of the two oscillation items in (2). If they are on the same scale or the natural oscillation dominates, there are still peaks in the residual spectra corresponding to natural oscillation frequencies. In this case, natural oscillations can be detected. Otherwise, if the forced oscillation dominates, then there may not be obvious peaks in the residual spectra, and the detection will be in favor of forced oscillation.

D. Algorithm for the Proposed RSA method

If there is oscillation in the PMU data $\hat{x}_r[k]$, whether the oscillation is natural or forced can be determined by detecting whether there are significant peaks in the spectra of the forecasting residuals. For reliable detection of spectral peaks, two metrics can be used jointly.

The first metric is the *residual spectra* c_{N_T}, which is

This article has been accepted for publication in a future issue of this journal, but has not been fully edited. Content may change prior to final publication. Citation information: DOI 10.1109/TSG.2017.2745494, IEEE Transactions on Smart Grid

defined in (22) as $S_e(\omega_n)$, the PSD of $e[k]$ at the oscillation frequency ω_n,

$$c_{N_T} = S_e(\omega_n). \quad (22)$$

The second metric is the residual slope $S(C)$ which is defined as

$$S(C) = slope\left(c_{N_{T1}}, c_{N_{T2}}, \cdots, c_{N_{TL}}\right) \quad (23.a)$$

This is the slope of the L residual spectra $C = \{c_{N_{T1}}, \cdots, c_{N_{TL}}\}$ with respect to the L lead times N_{Ti}, $i = 1, \cdots, L$. The slope can be calculated as the parameter a in the minimization of

$$\min_{\{a,b\}} \sum_{i=1}^{L} (c_{N_{Ti}} - aN_{Ti} - b)^2. \quad (23.b)$$

To determine this metric, a group of forecasting models with different lead times N_{Ti} are used, as shown in Fig. 2.

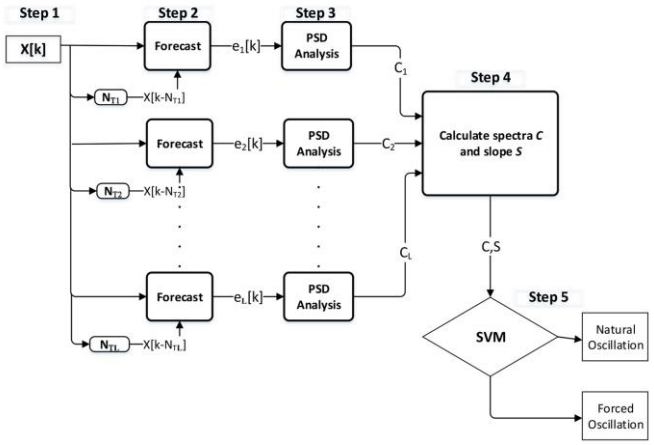

Fig. 2. Procedure of the proposed RSA method for distinguishing forced and natural oscillations.

Both the residual spectra c_{N_T} and the residual slope $S(C)$ of natural oscillations are often larger than those of forced oscillations for the same level of noise. The joint use of these two metrics makes the detection more reliable.

Based on the two metrics, an algorithm for the RSA method is outlined below, as illustrated by Fig. 2.

Algorithm for the RSA method
• **Step 1**. Collect data samples such as PMU data, and pre-process the data via detrending (removing DC) and normalization (for unit standard deviation).
• **Step 2**. For L forecasting delays $N_{T1} < \cdots < N_{TL}$, estimate the forecasting models and calculate the residuals $e[k]$.
• **Step 3**. Calculate PSDs of the residuals.
• **Step 4**. Calculate the two metrics. First, calculate residual spectra $C = \{c_{N_{T1}}, c_{N_{T2}}, \cdots, c_{N_{TL}}\}$ defined in (22) for each lead time. Then calculate residual slope S(C) in (23).
• **Step 5**. Compare the metrics with appropriate thresholds to classify the signals into forced or natural oscillations.

In step 5, classification can be conducted via SVM. Appropriate thresholds can be determined with some training data set and checked using validation data set.

IV. Performance Evaluation

In this section, case studies are carried out to evaluate the performance of the proposed RSA method. Both a simple artificial system and the 48-machine power system are used to generate simulation data with various natural and forced oscillations. When implementing the proposed algorithm, the MATLAB® function "oe.m" is used in step 2 to find the optimal forecasting model $g(x)$ and to calculate residuals. The Welch's method "pwelch.m" is used in step 3 to calculate the residual PSD. Many MATLAB® functions can be used to estimate the slope of C in step 4. The polynomial curve fitting function "polyfit.m" is used to calculate the slope $S(C)$ in step 4, where linear slope is obtained by choosing first order polynomials.

A. Case Study of a Simple Artificial System

To study some basic properties of the residual spectra c_{N_T}, the artificial system described by (24) is used to generate simulation data at 30 samples/s. The WGN $e(t)$ is used to mimic random perturbations to a power system. In order to generate the ambient noise, transfer function G_x(s) mimics the power system's low-pass features. Table I shows the three modes of G_x(s). The standard deviation of the ambient noise is set to 1.00.

$$x(t) = G_x(s)e(t) \quad (24a)$$

$$G_x(s) = \frac{20}{s+\sigma+0.4\cdot 2\pi j} + \frac{20}{s+\sigma-0.4\cdot 2\pi j} + \frac{30}{s+1.5+3.0\cdot 2\pi j} + \frac{30}{s+1.5-3.0\cdot 2\pi j} + \frac{40}{s+3.0+9.0\cdot 2\pi j} + \frac{40}{s+3.0-9.0\cdot 2\pi j} \quad (24b)$$

TABLE I. Modes of The Simple Ambient Nose Model

Index	*Frequency(Hz)*	*Damping Ratio*	*Residue*
1	0.4	ζ	20
2	3.0	7.9%	30
3	9.0	5.3%	40

To study the impact of the forecasting lead time on the *residual spectra* c_{N_T} under different damping, the damping ratio ζ of the 0.4 Hz mode is set to 0.19%, 2.78% and 7.90% by changing σ in (24b); and c_{N_T} is calculated as the PSD of the residual $e[k]$ normalized by the PSD of $x[k]$ at the oscillation frequency $\omega_n = 0.4$ Hz, $c_{N_T} = S_e(\omega_n)/S_x(\omega_n)$. The simulation results are shown in Fig. 3. It can be observed that the magnitude of c_{N_T} increases with the lead time. The observation is consistent with the analysis results presented in Section III.

Fig. 3 also shows the impact of the mode damping ratios on

This article has been accepted for publication in a future issue of this journal, but has not been fully edited. Content may change prior to final publication. Citation information: DOI 10.1109/TSG.2017.2745494, IEEE Transactions on Smart Grid

c_{N_T}. It can be observed that the slope of c_{N_T} decreases as the damping ratio increases, if the lead time is long enough (e.g., bigger than one second). This property suggests that the slope can be used to separate low damping natural oscillations from high damping natural oscillations.

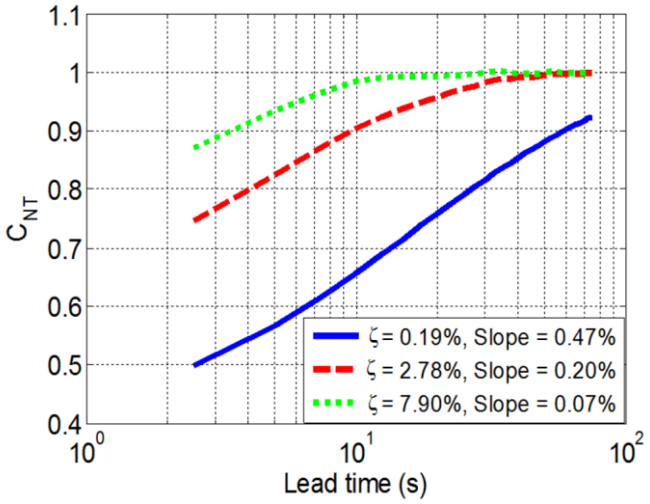

Fig. 3. Residual spectra c_{N_T} at $\omega_n = 0.4$ Hz as function of lead time N_T.

B. Case Study of the 48-Machine 140-Bus System

To study the performance of the proposed RSA method in more realistic power system applications, the 48-machine 140-bus model shown in Fig. 4 is used to generate PMU data. The major modes of the 48-machine model are presented in Table II. Power System Toolbox [28] is used to generate the simulation data for 200 seconds. For forced oscillations, a sinusoidal signal with a single frequency $\omega_0 = 0.4$ Hz and amplitude $A_1 = 0.1$ is injected into the system by modulating the shaft torque to mimic oscillation caused by vortex control [14] in a randomly picked generator.

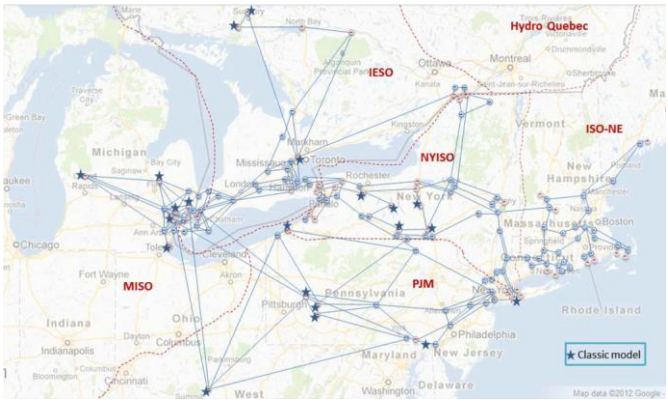

Fig. 4. Map of the NPCC 48-machine 140-bus system [29].

For natural oscillations, the damping coefficients of the generators are reduced to reach an unstable condition after a three-phase fault. The eigenvalue analysis method suggests that the dominant mode of the low-damped 48-machine model is at frequency of 0.6 Hz with the damping ratio of -3.8%. Fault location is randomly selected in the system. Preforming a time domain simulation using the non-linear model, the system's frequency deviation is shown in Fig. 5. In the figure, sustained oscillation at 0.6 Hz is observed. The sustained oscillation instead of growing oscillation (indicated by the negative damping mode) is observed because of the nonlinearity of the power system. Active and reactive loads of all the load buses are modulated by 5% of WGN to simulate the ambient noise. Frequency of bus 33 is recorded and used for the simulation study. With the 200 seconds of data, the analysis is performed on the last 150 seconds of data in order to focus on the steady state response.

TABLE II. MAJOR MODES OF THE 48-MACHINE MODEL

Mode Index	*Frequency (Hz)*	*Damping Ratio*
1	0.6	24 %
2	1.5	14 %
3	2.1	10 %

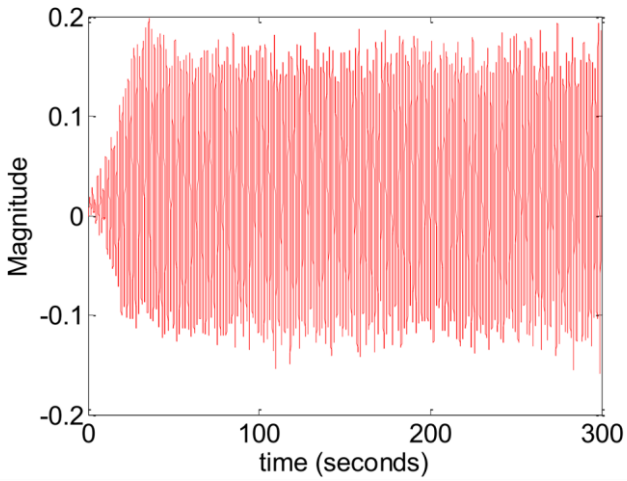

Fig. 5. Sustained oscillation observed at the voltage frequency of bus 33 for natural oscillations at 0.6 Hz.

The proposed RSA algorithm is applied to two data sets (i.e. one with forced oscillations and one with natural oscillations). PSDs with different lead times are estimated and plotted in Figs. 6 and 7. The symbol T_{osc} in the figures denotes the period of oscillations. The parameters for the Welch algorithm (step 3 in algorithm) are set as: discrete Fourier transform length (Nfft) 6144, 50% overlapping, and Hamming window with window size 2048.

As it can be seen in Fig. 6, there is a peak at 0.6 Hz for both the original signal and the forecasting residuals. In addition, the magnitude of the forecast residuals at oscillation frequency (0.6 Hz) increases as the lead time increases for the natural oscillations. In contrast, in the forced oscillation case in Fig. 7, there is no obvious peak at the oscillation frequency 0.4 Hz for the forecasting residuals. In addition, from Fig. 6, it can be observed that the spectra c_{N_T} at frequency 0.6 Hz increase with the forecasting lead time $n \times T_{osc}$. Therefore, the slope of the spectra defined by (23) is a reliable metric for distinguishing oscillations.

This article has been accepted for publication in a future issue of this journal, but has not been fully edited. Content may change prior to final publication. Citation information: DOI 10.1109/TSG.2017.2745494, IEEE Transactions on Smart Grid

To investigate the impact of higher order harmonics on the performance of the proposed method, the 2nd order harmonic, which has amplitude of 0.01 and phase shift of 90° degree, is added to the simulated forced oscillation. As it can be seen in Fig. 8, there is no obvious peak at the oscillation frequency 0.4 Hz for the forecasting residuals, which means that the higher order harmonic does not have any noticeable impact on the performance of the proposed method.

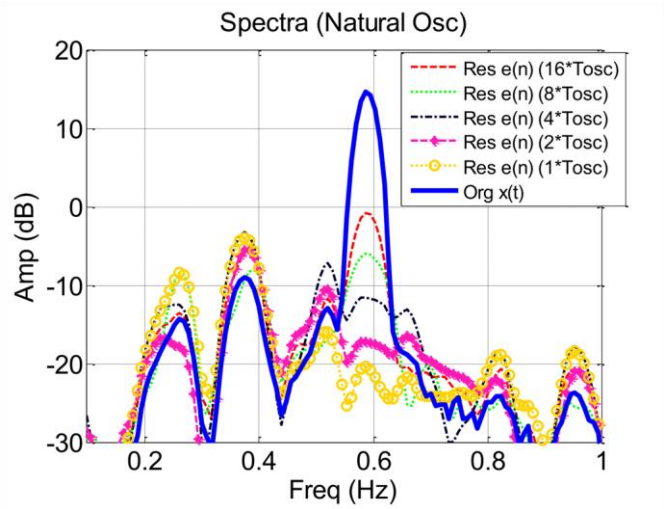

Fig. 6. PSDs of the original signal and the forecasting residuals in the **natural** oscillation case. (Here, "Res e(n) (16*Tosc)" means the residuals from the forecast model whose lead time is 16 times of oscillation periods; "Org x(t)" means the original data).

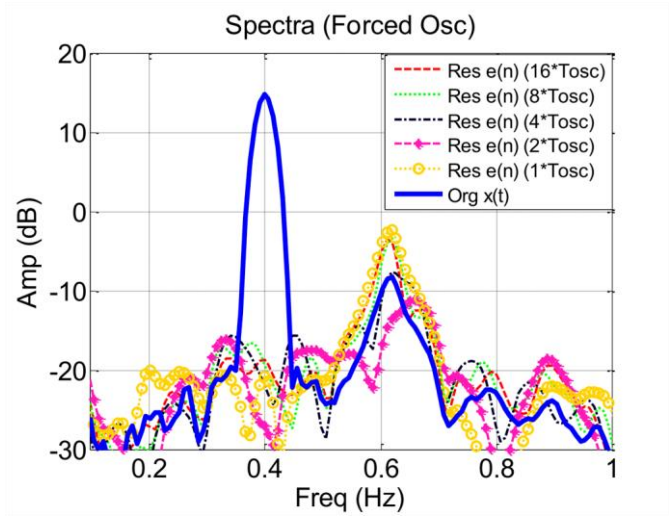

Fig. 7. PSDs of the original signal and the forecasting residuals in the **forced** oscillation case.

To evaluate the performance of SVM classification, Monte-Carlo simulations are conducted to generate 200 data sets (100 forced oscillations and 100 natural oscillations). Each data set contains 200 seconds of data. In addition, the data sets are divided into two groups: training and validation. The training and the validation data each consist of 50 sets of forced oscillations and 50 sets of natural oscillations. The proposed algorithm is applied to the training data to determine the classification thresholds. For the residual spectra, the mean magnitude of the residual spectra over L different lead-times is used in SVM because it results in a large classification margin. The oscillation classification results are plotted in Fig. 9. It can be observed that the proposed RSA method can correctly distinguish the forced and natural oscillations in both the training and validation data sets.

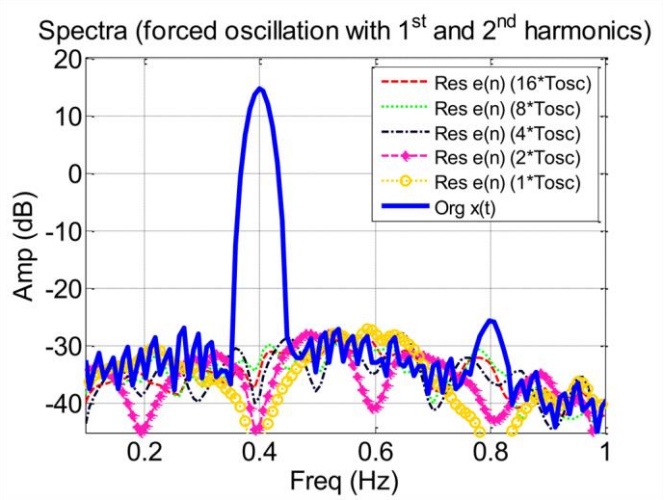

Fig. 8. PSDs of the original signal and the forecasting residuals in the **forced** oscillation case with 1st and 2nd order harmonics.

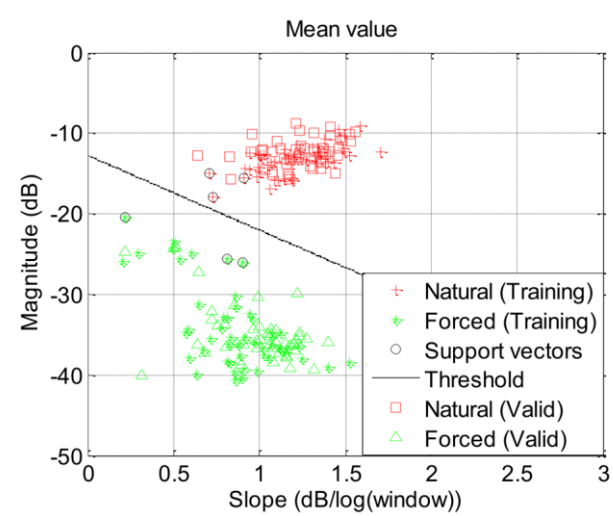

Fig. 9. SVM classification using the mean magnitudes and slopes of the spectra.

C. *Effects of Signal-to-Noise Ratio on Classification*

To study the influence of signal-to-noise ratio (SNR) on classification, the magnitudes of forced oscillations are varied (Amplitude = 0.05, 0.01, and 0.005) to obtain different SNRs (23.39 dB, 9.41 dB, and 3.39 dB, respectively), and 400 data sets of forced oscillations are simulated. Polynomial kernel of order 3 is used in SVM. The classification results are shown in Fig. 10. It can be observed that as the SNR decreases, the slope decreases and the spectra magnitude increases. The proposed method can correctly distinguish forced and natural oscillations.

D. *Comparison*

This subsection compares the proposed RSA method with

This article has been accepted for publication in a future issue of this journal, but has not been fully edited. Content may change prior to final publication. Citation information: DOI 10.1109/TSG.2017.2745494, IEEE Transactions on Smart Grid

the spectral method [24]. The idea in [24] is that the ratio of the PSDs between two different channels of PMU measurements (at oscillation frequency) does not change for natural oscillations, while this ratio increases significantly for forced oscillations. Using the same setting as subsection IV.B, a study is conducted for three different cases: 1) Natural oscillations with oscillation frequency at 0.6 Hz; 2) Forced oscillations with oscillation at 2.0 Hz; 3) Forced oscillations with oscillation frequency at 0.4 Hz (close to one of system's modes). The results are shown in Table III. Here, α_S is the ratio of PSDs between two different channels of PMU measurements when forced oscillations exist while α_N is the ratio of PSDs between two different measurement channels when forced oscillations do not exist.

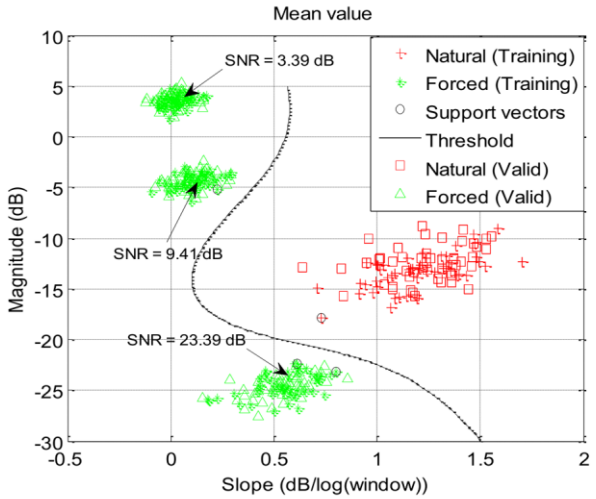

Fig. 10. SVM classification under various SNRs.

TABLE III. COMPARISON OF THE PROPOSED RSA METHOD WITH THE SPECTRAL METHOD [24].

Case Index	*1*	*2*	*3*
Oscillations Frequency (Hz)	*0.6*	*2.0*	*0.4*
α_S	3.5	47.4	1.5
α_N	4.0	0.9	1.7
Actual Oscillation type	Natural	Forced	Forced
Spectral Method[24]	Natural	Forced	**Natural**
Proposed RSA Method	Natural	Forced	Forced

As it can be seen in Table III, α_S and α_N are very close for **case 1,** so the spectral method [24] correctly identifies the case as natural oscillations. For case 2, the α_S and α_N at 2.0 Hz are not close to each other, so the spectral method correctly identifies it as forced oscillations. However, for case 3, the α_S and α_N are close to each other, which makes the spectral method misjudge it as a natural oscillation. Note that the misjudgment was because the spectral ratios of both ambient and oscillatory conditions converge to the same values (i.e., the relative mode shape) when the frequency of a forced oscillation is close to the frequency of a poorly damped system mode.

In contrast, the proposed RSA method is able to correctly determine the oscillation types in all the three cases. The magnitude and the slop of the residual spectra as well as the classification threshold are plotted in Fig. 11. The observation indicates that the proposed RSA method is more effective in distinguishing natural and forced oscillations than the spectral method, even when the forced oscillation frequency is close to the mode frequency.

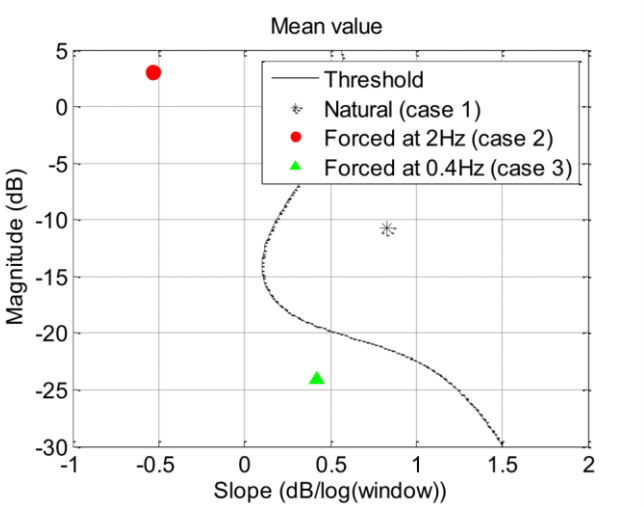

Fig. 11. The proposed RSA method can correctly distinguish the oscillations.

E. Case Study using Field Measurement Data

To test its applicability in a real-life example, the proposed RSA method is applied to the field measurement data during forced and natural oscillations. Note that the oscillation frequency and magnitudes in a real world often change gradually. To accommodate the gradual changes, a sliding window approach is used to apply the proposed RSA method on the measurement data within a window, one block at a time, to calculate the residuals.

The natural oscillation data shown in Fig. 12 were recorded right before the power outage happened in WECC system on August 10, 1996 [1]. It was determined that the outage was caused by a natural oscillation mode at 0.25 Hz mode that grew out of control and caused the power outage in WECC system [1] [26]. Modal analysis carried out by [26] also showed that there was a sustained oscillation at 0.25 Hz between 450 s and 650 s. The proposed RSA method is applied to the normalized data set with sliding window side of $1*T_{osc}$ (i.e., 4.0 s). The resulting spectra is summarized in Fig. 13. It can be observed that at 0.25 Hz, the magnitudes of the residual spectra increase when the time delay increases. Also, the magnitudes of residual spectra are not significantly smaller than the original spectra. Based on the proposed RSA method, the observation indicates that the oscillation is a natural oscillation.

The forced oscillation data shown in Fig. 14 were retrieved from the website of North American Synchrophasor Initiative (NASPI) [30], which was provided by NASPI as an example of forced oscillation. Spectral analysis showed that that there was a sustained oscillation at 1.25 Hz between 250 s and 450 s. The proposed RSA method is applied to the normalized data set with sliding window side of $1*T_{osc}$ (i.e., 0.8 s). The resulting spectra is summarized in Fig. 15. It can be observed that at 1.25 Hz, the magnitudes of the residual spectra do not

This article has been accepted for publication in a future issue of this journal, but has not been fully edited. Content may change prior to final publication. Citation information: DOI 10.1109/TSG.2017.2745494, IEEE Transactions on Smart Grid

increase proportionally with their time delay. For example, the magnitude of the residual spectra with time delay of $2*T_{osc}$ is larger than that of $16*T_{osc}$. Also, the magnitudes of residual spectra are significantly smaller than the original spectra. Based on the proposed RSA method, the observation indicates that the oscillation is a forced oscillation.

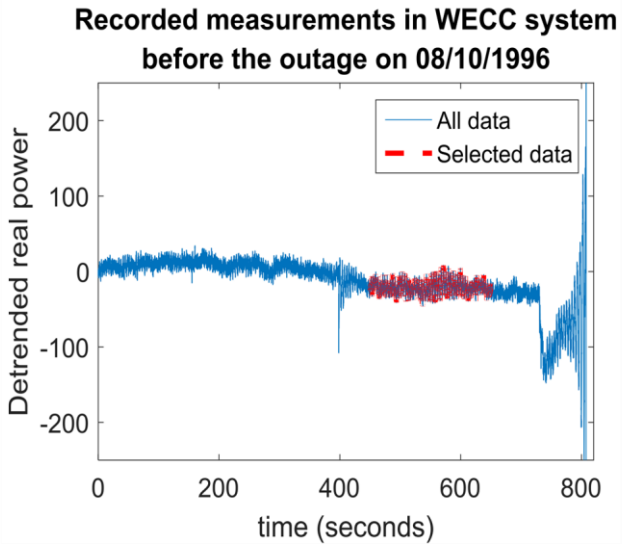

Fig. 12. Detrended real power on a major transmission line in the WECC system right before the power outage on 08/10/1996.

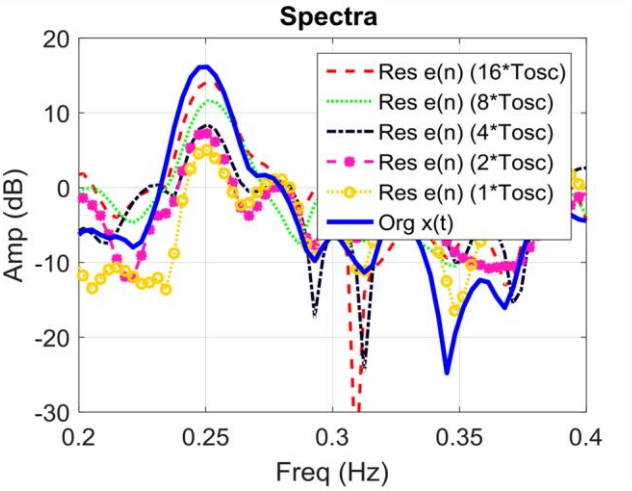

Fig. 13 PSDs of the original signal and the forecasting residuals in the natural oscillation that happened in the WECC system before the power outage on 08/10/1996.

V. Conclusion and Future Work

This paper proposes a residual spectrum analysis (RSA) method to distinguish natural oscillations from forced oscillations using the spectra of the forecasting residuals. For natural oscillations, since the system response is dominated by the random sinusoidal signal, the spectra of the forecasting residuals peak at the oscillation frequency. The magnitude of the peak increases with the lead time of the forecast model. In contrast, for forced oscillations, since the system response is dominated by the deterministic sinusoidal signal, the spectra of the forecasting residuals do not necessarily have peaks at the oscillation frequency. The proposed RSA method exploits such unique features to distinguish forced and natural oscillations. An algorithm is developed to estimate the forecasting residuals, calculate the spectra, and use SVMs to classify oscillations. Simulations over both a simple artificial system model and the 48-machine model show that the proposed RSA method can effectively distinguish forced oscillations from natural oscillations, even when the forced oscillation frequency is close to system modes.

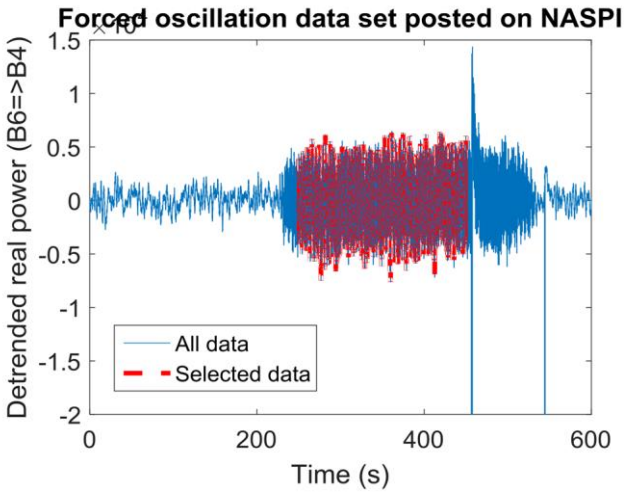

Fig. 14. Detrended real power from bus6 to bus4 during a sustained forced oscillation event posted on the NASPI website.

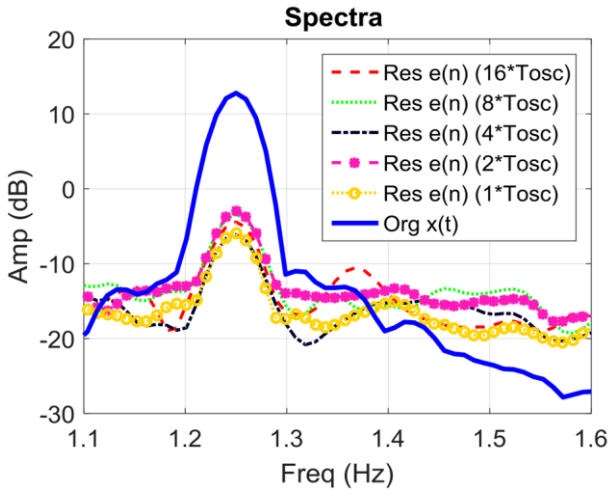

Fig. 15. PSDs of the original signal and the forecasting residuals in the forced oscillation case posted on the NASPI website.

VI. References

[1] D. N. Kosterev, C. W. Taylor, and W. A. Mittelstadt, "Model validation for the August 10, 1996 WSCC system outage," *IEEE Transactions on Power Systems.*, vol. 14, no. 3, pp. 967–979, 1999.

[2] M. Magdy and F. Coowar, "Frequency domain analysis of power system forced oscillations," *IEE Proceeding C (Generation, Transmission and Distribution)* , vol. 137, no. 4, pp. 261–268, 1990.

[3] C. Vournas and N. Krassas, "Analysis of forced oscillations in a multimachine power system," *Control 1991*, vol. 2, pp. 443–448, 1991.

[4] P. Kundur, *Power System Stability and Control*. New York: McGraw-Hill, 1994.

[5] W. Du, H. F. Wang, and R. Dunn, "Power system oscillation stability and control by FACTS and ESS - A survey," *1st Int. Conf. Sustain. Power Gener. Supply,(SUPERGEN '09)*, pp. 1–13, 2009.

[6] N. Zhou, Z. Huang, F. Tuffner, S. Jin, J. Lin, and M. Hauer,

Osscillation Detection and Analysis. Pacific Northwest National Laboratory, Project Report, Aug. 2010.

[7] A. A. Girgis and F. M. Ham, "A quantitative study of pitfalls in the FFT," *IEEE Trans. on Aerospace and Electronic Systems* , vol. AES-16, no. 4, pp. 434–439, 1980.

[8] C. J. Demeure and L. L. Scharf, "Initial results in Prony analysis of power system response signals," *IEEE Trans. on power systems.*, vol. 5, no. 1, pp. 80–89, 1990.

[9] T. K. Sarkar and O. Pereira, "Using the matrix pencil method to estimate the parameters of a sum of complex exponentials," *IEEE Antennas and Propagation Magazine*., vol. 37, no. 1, pp. 48–55, 1995.

[10] D. J. Trudnowski and J. W. Pierre, "Overview of algorithms for estimating swing modes from measured responses," *Power & Energy Society General Meeting (PES '09)*, pp. 1–8, 2009.

[11] L. Vanfretti, L. Dosiek, J. W. Pierre, D. Trudnowski, J. H. Chow, R. Garcia-Valle, and U. Aliyu, "Application of ambient analysis techniques for the estimation of electromechanical oscillations from measured PMU data in four different power systems," *International Transactions on Electrical Energy Systems.*, vol. 21, no. 4, pp. 1640–1656, 2011.

[12] J. Van Ness, "Response of large power systems to cyclic load variations," *IEEE Trans. on Power Apparatus and Systems.*, no. 7, pp. 723–727, 1966.

[13] J. Ma, P. Zhang, H. J. Fu, B. Bo, and Z. Y. Dong, "Application of phasor measurement unit on locating disturbance source for low-frequency oscillation," *IEEE Trans. on Smart Grid.*, vol. 1, no. 3, pp. 340–346, 2010.

[14] S. A. N. Sarmadi and V. Venkatasubramanian, "Inter-area resonance in power systems from forced oscillations," *IEEE Trans. on Power Systems*, vol. 31, no. 1, pp. 378–386, 2015.

[15] N. Zhou and J. Dagle, "Initial results in using a self-coherence method for detecting sustained oscillations," *IEEE Trans. on Power Systems.*, vol. 30, no. 1, pp. 522–530, 2015.

[16] M. Ghorbaniparvar and N. Zhou, "Bootstrap-based hypothesis test for detecting sustained oscillations," *2015 IEEE Power Energy Soc. Gen. Meet. (PES '15)*, pp. 1–5, 2015.

[17] M. Ghorbaniparvar, "A survey on forced oscillations in power system," *J. Mod. Power Syst. Clear Energy*, in press.

[18] G. Rogers, *Power System Oscillations*. Norwell, Ma, USA: Kluwer, 2000.

[19] E. V. Larsen and D. A. Swann, "Applying power system stabilizers, Part I: Basic Concepts," *IEEE Trans. Power Appar. Syst.*, vol. PAS-100,, no. 6, p. 3017-3024, 1981.

[20] A. Silverstein, *Diagnosing Equipment Health and Mis-operations with PMU Data*. 2015.

[21] L. Vanfretti, S. Bengtsson, V. H. Aarstrand, and J. O. Gjerde, "Applications of spectral analysis techniques for estimating the Nordic grid's low frequency electromechanical oscillations," *IFAC Proceedings*, vol. 45, no. 16, pp. 1001–1006, 2012.

[22] L. Vanfretti, S. Bengtsson, V. S. Peric, and J. O. Gjerde, "Effects of forced oscillations in power system damping estimation," *2012 IEEE Int. Work. Appl. Meas. Power Syst. (AMPS 2012)*, pp. 59–64, 2012.

[23] J. Liu, W. Yao, J. Wen, H. He, and X. Zheng, "Active power oscillation property classification of electric power systems based on SVM," *Journal of Applied Mathematics*, 2014.

[24] R. Xie and D. Trudnowski, "Distinguishing features of natural and forced oscillations," *2015 IEEE Power Eng. Soc. Gen. Meet.*, pp. 1–5, 2015.

[25] X. Wang and K. Turitsyn, "Data-driven diagnostics of mechanism and source of sustained oscillations," *IEEE Trans. on Power Systems.*, vol. 31, no. 5, pp. 4036–4046, 2016.

[26] J. F. Hauer, D. J. Trudnowski, and J. G. Desteese, "A perspective on WAMS analysis tools for tracking of oscillatory dynamics," *2007 IEEE Power Eng. Soc. Gen. Meet. (PES'2007)*, 2007.

[27] J. Follum and J. W. Pierre, "Initial results in the detection and estimation of forced oscillations in power systems," *2013 North Am. Power Symp.*, pp. 1–6, 2013.

[28] J. H. Chow and K. W. Cheung, "A toolbox for power system dynamics and control engineering education and research," *IEEE Trans. on Power Systems*, vol. 7, no. 4, pp. 1559–1564, 1992.

[29] J. Qi, K. Sun, J. Wang, and H. Liu, "Dynamic state estimation for multi-machine power system by unscented Kalman filter with enhanced numerical stability," *IEEE Trans. on Smart Grid*, in press.

[30] R. Xie, D. J. Trudnowski, "Distinguishing between natural and forced oscillations using a cross-spectrum index, " *2017 IEEE Power Eng. Soc. Gen. Meet.*, Chicago, IL, USA, July 16-21, 2017.

[30] Oscillation Detection and Voltage Stability Tools Technical Workshop, *Oscillation Analysis Test Case 2*, available online at https://www.naspi.org/node/440, last access on 08/10/2017.

Mohammadreza Ghorbaniparvar (S'15) is currently a graduate student at the Department of Electrical and Computer Engineering, State University of New York at Binghamton, Binghamton, NY. His research interests include digital signal processing, power system dynamic performance, oscillation detection, smart grid, and demand side management. He is a student member of the IEEE Power and Energy Society (PES) and IEEE Signal Processing Society (SPC).

Ning Zhou (S'01–M'05–SM'08) is an assistant professor at the Electrical and Computer Engineering Department of the Binghamton University. He was with Pacific Northwest National Laboratory (PNNL) as a power system engineer from 2005 to 2013. In 2005, he received his Ph.D. in electrical engineering with a minor in statistics from the University of Wyoming. His research interests include power system dynamics and statistical signal processing. Dr. Zhou is a senior member of the IEEE Power and Energy Society (PES).

Xiaohua Li (M'00-SM'06) received the B.S. and M.S. degrees from Shanghai Jiao Tong University, Shanghai, China, in 1992 and 1995, respectively. He received the Ph.D. degree in Electrical Engineering from the University of Cincinnati, Cincinnati, OH, in 2000. He was an assistant professor from 2000 to 2006, and has been an Associate Professor since 2006, both with the Department of Electrical and Computer Engineering, State University of New York at Binghamton, Binghamton, NY. His research interests are in the fields of signal processing, machine learning, wireless communications, and wireless information assurance.

Daniel J. Trudnowski (M'91–SM'99–F'09) received the B.S. degree in engineering science from Montana Tech, Butte, in 1986, and the M.S. and Ph.D. degrees in electrical engineering from Montana State University in 1988 and 1991, respectively. From 1991–1995, he was with Battelle, Pacific Northwest National Laboratory where he was a senior research engineer. In 1995, he joined the Montana Tech where he is currently a professor and head of the Electrical Engineering Department. His research activities over the past 20 years have primarily focused on problems related to power system dynamics and controls. Dr. Trudnowski is a member of the IEEE Power System and Control System Societies and is a registered professional engineer in the state of Montana.

Ruichao Xie (S'15) received his Master's degree in Electrical Engineering from Montana Tech of the University of Montana, USA, in 2015. He was a research associate at the same school during 2015-2017. He is currently pursuing the Ph.D. degree in Electrical Engineering at Laval University, Canada. His research interests are power system dynamic stability and controls.